LUNAR INFLUENCE ON EQUATORIAL ATMOSPHERIC ANGULAR MOMENTUM

C. BIZOUARD[1], L. ZOTOV[2], N. SIDORENKOV[3]
[1] SYRTE, Observatoire de Paris, CNRS/UPMC
61, avenue de l'Observatoire, 75014 Paris, France
e-mail: christian.bizouard@obsm.fr
[2] Sternberg Astronomical Institute of Moscow State University
Moscow, Russia
e-mail: wolftempus@gmail.com
[3] Hydrometeorological Centre of Russia / Global Atmospheric Circulation Laboratory
Moscow, Russia
e-mail: sidorenkov@mecom.ru

ABSTRACT This study investigates the relationship between the equatorial atmospheric angular momentum oscillation in the non-rotating frame and lunar tidal potential. Between 2 and 30 days, the corresponding equatorial component is mostly constituted of prograde circular motions, especially of a harmonic at 13.6 days, and of a weekly broad band variation. A simple equilibrium tide model explains the 13.6-day pressure term as result of the O_1 lunar tide; the tidal lunar origin of the whole band from 2 to 30 days is attested by specific features, not occurring for seasonal band dominated by the solar thermal effect.

1. INTRODUCTION

The Equatorial Atmospheric Angular Momentum (EAM) displays prominent quasi-diurnal clockwise variations at 24 h (S_1), 24.07 h (P_1) and 23.93 h (K_1), commonly interpreted as the effect of diurnal solar thermal heating (24 h) subject to a yearly amplitude modulation (Bizouard et al., 1998). It also presents a minor but sharp 25.82-hour peak (Brzeziński et al., 2002) evasively attributed to the O_1 lunar tesseral tide, considering the absence of thermal processes at this frequency. This paper deepens the insight into this signal by an analysis of equatorial AAM variations from 2 to 30 days in the non-rotating frame.

2. BASIC DEFINITIONS

Let H_i be the Cartesian components of the Atmospheric Angular Momentum vector in the Terrestrial Reference Frame (TRF), $C = 8.0370\,10^{37}$ kg m^2 the mean axial moment of inertia, $A = 8.0101\,10^{37}$ kg m^2 the mean equatorial moment of inertia, $\Omega = 2\pi\,1.002738$ rad/day the mean stellar angular frequency. At sub-secular time scales, polar motion (and by extension nutation) are commonly investigated by the linear Liouville equations, where the equatorial excitation of any surface fluid layer maps into a non-dimensional terrestrial quantity $\chi = \chi_1 + i\chi_2$ of the angular momentum of this layer with $\chi_1 = H_1/((C-A)\Omega)$, $\chi_2 = H_2/((C-A)\Omega)$. The χ_i are called Equatorial Angular Momentum Functions (EAMF) and are composed of two terms: i) the first, produced by the rotation of the air mass distribution, can be computed from surface pressure data, and is usually called *pressure term*; ii) the second, caused by the winds, is proportional to the relative angular momentum of the atmosphere, and might be denoted as *wind term* (Barnes et al., 1983). Note that, in order to account for Earth's non-rigidity in the Liouville equations, the AMF have to be multiplied by appropriate coefficients close to 1, yielding the so-called Effective EAMF. Brzeziński (1994) introduced the concept of Celestial Equatorial Angular Momentum (CEAM) defined by

$$\chi' = -\chi e^{i\theta(t)}\,, \tag{1}$$

where $\theta(t) = \theta(TAI_0) + \Omega(TAI - TAI_0)$ is the uniformly varying rotation angle with TAI_0 being a conventionally chosen instant of TAI (IERS Conventions, 2010). Whereas the diurnal band is squeezed in a frequency band around 24 h in the TRF, the corresponding periodicities of the CEAM stretch

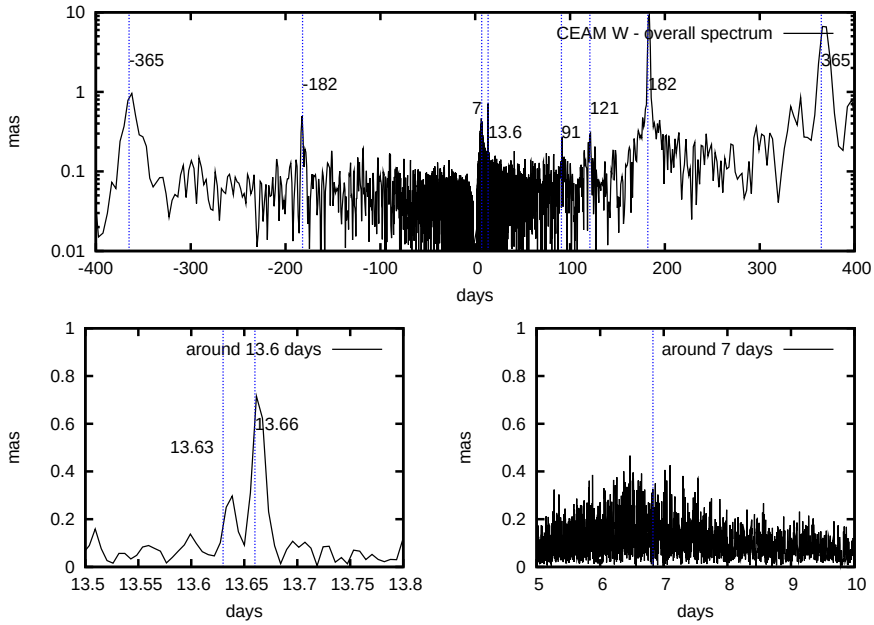

Figure 1: Amplitude spectrum of the wind term of the Celestial Angular Momentum over the period 1949-2012. Data source: NCEP/NCAR.

from 2 days to several years with respect to the non-rotating reference frame: any diurnal component of frequency $\sigma = -\Omega + \sigma'$ with $\sigma' \ll \Omega$ is mapped to a long periodic celestial component of frequency σ'.

3. ANALYSIS OF THE CEAM

Using 6-hourly EAMF estimates from the reanalysis model of NCEP/NCAR (National Center for Environmental Prediction / National Center of Atmospheric Research) over the period 1949−2013, as provided by the Global Geophysical Fluids Center of the IERS (SBA, 2014), we computed the associated CEAM according to (1) for both pressure and wind terms. Prior to demodulation, we removed the long term components (periods larger than 2 days) of the AAM. After application of (1), a low band pass filter was used to eliminate residual diurnal/sub-diurnal signal content and to obtain the celestial excitation limited to periods larger than 2 days, corresponding to the precession-nutation frequency band.

The complex Fourier spectrum of the obtained wind term of CEAM is displayed in Fig. 1 (pressure term presents the same spectral peaks with lower amplitude). Casting aside the peaks with periods above 100 days widely characterised by numerous studies, we focus on the rapid band of the CEAM between 2 days and 30 days, of which the spectral zoom clearly unveils a harmonic at +13.6 days (25.8 h in the TRF) and a broad band peak around +7 days (28 h in the TRF).

After applying an appropriate high band pass filter, this band is isolated in time domain and shown over 130 days (from MJD 50000 to MJD 50130) in Fig. 2 for both wind terms in X and Y components as well as the full Non Inverted Barometer (NIB) pressure terms. It is remarkable that, for X and Y coordinates, wind and pressure terms are evidently proportional. Throughout the period 1949−2014 correlations amount to 0.57 for both X components and Y components and linear regression gives $\chi'_w \sim 2.1\chi'_p$. The detected proportionality appears to be a feature of the short term CEAM from 2 days to 1 month; it does not extend to the complementary spectral bands, ranging from 1 month to several years, where correlations between pressure and wind terms drop to 0.1. Another striking feature distinguishing the 2−30 day band from other parts of the spectrum is the fact that contributions of Northern and Southern hemisphere to the wind terms have synchronous variations, as evidenced by Fig. 2.

The torque that the atmosphere exerts on the solid Earth is composed of the bulge torque $\vec{\Gamma}_b$ acting on the equatorial bulge because of pressure and gravitational forces, and of a local torque $\vec{\Gamma}_l$ caused by pressure on the local topography as well as the friction drag on Earth's surface. In the non-rotating frame we have the following complex quantities: $H'_{w/p}$ for the equatorial wind/pressure term, Γ'_l for the local torque, Γ'_b for the bulge torque, Γ'_{ext} for the external gravitational torque on the atmosphere. As shown

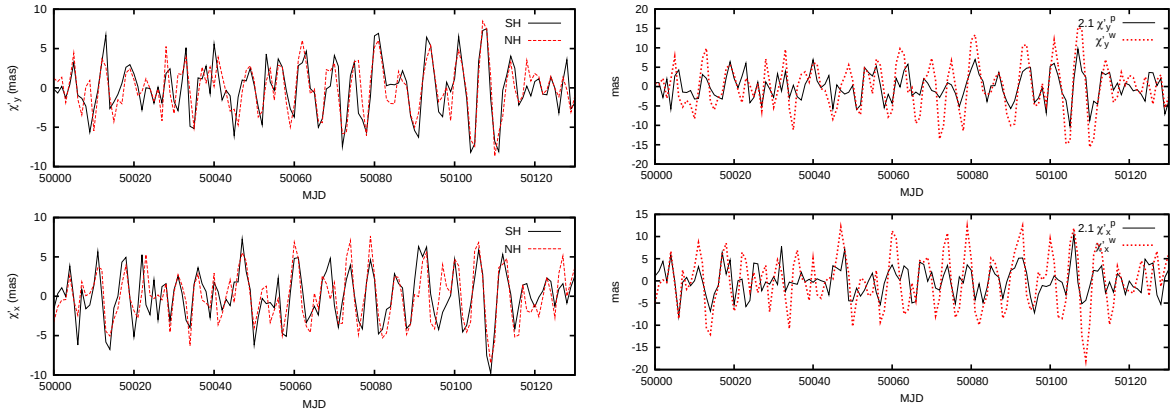

Figure 2: Left panel: contributions of the Southern Hemisphere (SH) and Northern Hemisphere (NH) to the wind term in χ'_X (bottom) and χ'_Y (top) for the 2−30 day band. Right panel: components X and Y of the Celestial Atmospheric Angular Momentum for wind term χ_w and NIB pressure term χ_p multiplied by 2.1 (linear regression coefficient from 1949 to 2014) computed from CEAM series after eliminating long term periods above 1 month. Time series over 130 days commencing at MJD 50000 (10/10, 1995).

in (Bizouard et al., 2014), law of the angular momentum allows to established in frequency domain that

$$1 - \frac{\sigma'}{\Omega} - \frac{\sigma'}{\Omega}\frac{\hat{H}'_w}{\hat{H}'_p} = \frac{-\hat{\Gamma}'_l + \hat{\Gamma}'_{ext}}{\hat{\Gamma}'_b} \ , \tag{2}$$

where the sign " ˆ " corresponds to the Fourier transform. If the residual torque $-\hat{\Gamma}'_l + \hat{\Gamma}'_{ext}$ is much smaller than the bulge torque Γ'_b then

$$\hat{H}'_w \approx \frac{\Omega - \sigma'}{\sigma'}\hat{H}'_p \ . \tag{3}$$

For positive angular frequencies σ' of the filtered CEAM, with periods from 2 days to 1 month, we have $1/30\,\Omega \leq \sigma' \leq 1/2\,\Omega$ (the retrograde part of the spectrum is much smaller); so, according to (3) pressure and wind terms become almost proportional. This is in contrast with the seasonal band (S_1 in the TRF) where the smallness of the local torque with respect to the bulge torque is not satisfied (Marcus et al., 2004). Considering for the lunar tidal band a typical magnitude of $|\chi'_p| \sim 0.2$ mas (see fit of section 4), the bulge torque magnitude, given by $|\Gamma'_b| = \Omega^2(C-A)|\chi'_p|$ (Marcus et al., 2004), amounts to $\sim 1.5\,10^{18}$ Nm. According to (Bizouard and Lambert, 2001), the diurnal external torque Γ'_{ext} is at most $\sim 10^{17}$ Nm, which is at least 10 times smaller than the equatorial bulge torque $\Omega|H'_p|$. Hence, as far as the local torque does not exceed the order of magnitude of the external torque, the above condition holds.

4. TIDAL ORIGIN OF THE 13.6-DAY TERM AND QUASI-WEEKLY BAND

The most natural hypothesis for the origin of the 13.66 day peak is the diurnal tidal wave O_1 determined by the Delaunay argument $2(F+\overline{\Omega})$ in the non-rotating frame, with $F = \overline{\omega} + l$ being the sum of the perigee argument $\overline{\omega}$ and the mean anomaly l, and $\overline{\Omega}$ being the longitude of the ascending node of the Moon on the ecliptic plane. As expected from tidal theory, the main peak is accompanied by a side-lobe at 13.63 days having the argument $2F + \overline{\Omega}$. These two components differ by the frequency $\overline{\Omega}$ of the displacement of the ascending node of the Moon, that is 1/18.6 cpy (cycles/year). The fact that we observe both of these peaks in CEAM substantiates the tesseral lunar influence on CEAM, in particular on the wind component. The celestial oscillations of arguments $\Phi_1 = 2F + 2\overline{\Omega}$ (13.66 days) and $\Phi_2 = 2F + \overline{\Omega}$ (13.63 days) are fitted by a least-squares method to the model $\chi' = \sum_{j=1}^{2}(m_c^j + i m_s^j)e^{i(\phi_j + \pi/2)}$. For the period 1949−2013 we obtain

$$\begin{aligned}
\chi'^{IB}_p[mas] &= (0.05 - i0.02)\, e^{i(\phi_1+\pi/2)} + (0.02 - i0.00)\, e^{i(\phi_2+\pi/2)} \\
\chi'^{NIB}_p[mas] &= (0.17 - i0.06)\, e^{i(\phi_1+\pi/2)} + (0.06 - i0.01)\, e^{i(\phi_2+\pi/2)} \\
\chi'_w[mas] &= (0.73 - i0.04)\, e^{i(\phi_1+\pi/2)} + (0.23 - i0.01)\, e^{i(\phi_2+\pi/2)}
\end{aligned} \tag{4}$$

The m_s terms are small relatively to m_c, except for the IB term. Disregarding the IB solution, the harmonic coefficients are therefore almost in phase with the tidal wave of argument $\phi_i+\pi/2$, confirming the proportionality of wind and pressure terms at this period and supporting their common tidal gravitational cause. The ratio $\chi'_w/\chi'^{NIB}_p = H'_w/H'_p \sim 4$ for both tidal frequencies does not match the numerical value of the condition (3), namely $H'_w/H'_p = 13.6 - 1 \sim 13$. On the other hand the ratio $\chi'_w/\chi'^{IB}_p \approx 14$ much better fits the expected ratio of 12.6, as if the effective pressure term around the O_1 frequency was the one restricted to continents and a static IB ocean. This is quite peculiar, since an IB response of the oceans is generally observed above 10 days but not at diurnal periods in the TRF.

The mere consideration that the tidal O_1 oscillation is at equilibrium accounts for both the amplitude and the phase of the NIB pressure term (Bizouard et al., 2014). If the hydrostatic assumption is true for surface pressure, tidal winds do not blow at Earth's surface, but at high altitudes. As tidal lunar variation of the horizontal wind have never been indeed reported in the low troposphere, tidal winds do not produce any notable friction torque. On the other hand, a tesseral tidal pressure field exerts a torque on the bulge but cannot contribute to the topographic torque, which results from spherical harmonics of degree higher than 3 (Bizouard, 2014). Thus the tidal atmospheric circulation does not contribute significantly to the local torque, in accordance with condition (3), and it accounts for the proportionality of χ'_w and χ'_p.

The broad band peak between 5 and 8 days is much more powerful than the thin peaks around 13.6 days, showing episodes with an amplitude of 10 mas. Some studies like (Brzeziński et al., 2002) attribute this weekly signal to the retrograde Rossby-Haurwitz atmospheric normal mode Ψ^1_1, having in the TRF the geometry of a spherical harmonic $\cos(\phi)e^{i\lambda}$ (ϕ is the latitude, λ is the longitude) propagating to the west. In the non-rotating frame, this resonant mode propagates from the west to the east as the Moon, and with an averaged period of ~ 7 days it could be amplified at planetary scale by the minor lunar tides around 7.09 days at least 100 times smaller than O_1. Moreover, at quasi-weekly periods ($\sigma'/\Omega \approx 1/7$) the ratio $\chi'_w/\chi'^{NIB}_p \approx 5.8$ fits the condition (3) reading $H'_w/H'_p \approx 7 - 1 = 6$, and is thus valid for the full pressure term in contrast to what is observed at 13.6 days.

5. CONCLUSION

Our quintessential conclusion is as follows: from 2 to 30 days in the CRF (24.8 h to 48 h in the TRF) the retrograde equatorial atmospheric angular momentum variations are triggered by the Moon. In order to observe a possible effect on nutation, improvements of the VLBI/GNSS data processing as well as optimized observation schedules are required.

6. REFERENCES

Barnes, R.T.H., Hide, R., White, A.A., Wilson, C.A., 1983, "Atmospheric angular momentum fluctuations, length-of-day changes and polar motion", Proc. R. Soc. London A ,387, pp. 31–73.

Bizouard, C., Brzeziński A., Petrov, S., 1998, "Diurnal atmospheric forcing and temporal variations of the nutation amplitudes", J. Geodesy, 72, pp. 561–577.

Bizouard, C., Lambert, S., 2001, "Lunisolar torque on the atmosphere and Earth's rotation", Planetary and Space Science, 50(3), pp. 323–333.

Bizouard, C., 2014, "Le mouvement du pôle de l'heure au siècle", PAF, 284 pp.

Bizouard, C., Zotov, L., Sidorenkov, N., 2014, "Lunar influence on equatorial angular momentum", J. Geophys. Res.: Atmosphere, 119, pp. 11,920–11,931, DOI: 10.1002/2014JD022240.

Brzeziński, A., 1994, "Polar motion excitation by variations of the effective angular momentum function, II: Extended model", Manuscripta Geodaetica, 19, 157–171.

Brzeziński, A., Bizouard, C., Petrov, S., 2002, "Influence of the atmosphere on Earth rotation: what new can be learnt from the recent atmospheric angular momentum estimates?" Surv. Geophys., 23, pp. 33–69.

IERS Conventions, 2010, G. Petit, B. Luzum (eds.), IERS Technical Note 36, Frankfurt am Main: Verlag des Bundesamts für Kartographie und Geodäsie.

Marcus, S., de Viron, O., Dickey, J., 2004, "Atmospheric contributions to Earth Nutation: Geodetic constraints and limitations of the torque approach", Atmospheric sciences, 61, pp. 352–356.

SBA, 2014, website of the IERS Special Bureau for the Atmosphere `http://ftp.aer.com/pub/anon_collaborations/sba/`.